Electronic Transactions on Numerical Analysis.
Volume 63, pp. 424–451, 2025 (Supplementary Material).

ISSN 1068–9613.
DOI: 10.1553/etna_vol63s424

ETNA
Kent State University and
Johann Radon Institute (RICAM)

SUPPLEMENTARY MATERIAL TO: REVISITING THE NOTION OF APPROXIMATING CLASS OF SEQUENCES FOR HANDLING APPROXIMATED PDES ON MOVING OR UNBOUNDED DOMAINS

ANDREA ADRIANI[†], ALEC JACOPO ALMO SCHIAVONI-PIAZZA[‡], STEFANO SERRA-CAPIZZANO[§], AND CRISTINA TABLINO-POSSIO[¶]

Abstract. This note represents supplementary material to the article [Electron. Trans. Numer. Anal., 63 (2025), pp. 424–451].

https://etna.ricam.oeaw.ac.at/volumes/2021-2030/vol63/abstract.php?pages=424-451

1. Premises. The present document represents a supplementary material, associated with the paper [1], where we report a great deal of numerical experiments and visualizations, corroborating its theoretical findings and giving information on the value of the new concept of g.a.c.s. given in [1, Definition 2.1] with respect to the standard a.c.s. concept [6].

Let us consider a domain $\Omega = \{(x,y) \in \mathbb{R} : x > 0, y > 0 \text{ and } y < g(x)\}$ with

$$g(x) = \begin{cases} 1 & x < 1, \\ \frac{1}{x^2} & x \geq 1, \end{cases}$$

and the elliptic problems

$$\begin{aligned} -\Delta u &= v \quad \text{on } \Omega, \\ u &= 0 \quad \text{on } \partial\Omega, \end{aligned} \tag{1.1}$$

and

$$\begin{aligned} \operatorname{div}(-a\nabla u) &= v \quad \text{on } \Omega, \\ u &= 0 \quad \text{on } \partial\Omega, \end{aligned} \tag{1.2}$$

where $a(x,y)$ is a positive non-degenerate variable coefficient on Ω. We focus on a few discretization techniques for the approximation of the solution, namely standard centered finite differences of order two (or equivalently, P_1-finite elements), Q_1-finite elements, and P_2-finite elements. With reference to Remark 4.3 in the article, we observed that the conditioning of the resulting matrices grows as $N^{\frac{2}{d}}$, with N being the matrix size and d being the dimensionality. This is due to the minimal eigenvalue, which converges to zero as $N^{-\frac{2}{d}}$ (see [4, 5, 2] for the pure Toeplitz setting and [3, 7] for the variable-coefficient case), and the related property can

[†]University of Rome Tor Vergata, Via della Ricerca Scientifica 1, 00133 Roma, Italy, Department of Science and High Technology, Division of Mathematics, University of Insubria, Via Valleggio 11, 22100 Como, Italy (adriani@mat.uniroma2.it, andrea.adriani@uninsubria.it).

[‡]Scuola Internazionale Superiore di Studi Avanzati, Via Bonomea 265, 34136 Trieste, Italy, Department of Mathematics, Computer Science, and Geosciences, University of Trieste, via Valerio 12/1, 34127 Trieste, Italy (aschiavo@sissa.it).

[§]Department of Science and High Technology, Division of Mathematics, University of Insubria, Via Valleggio 11, 22100 Como, Italy, Department of Information Technology, Division of Scientific Computing, Uppsala University, Box 337, SE-751 05, Uppsala, Sweden
(s.serracapizzano@uninsubria.it, stefano.serra@it.uu.se).

[¶]Corresponding author. Department of Mathematics and Applications, University of Milano - Bicocca, via Cozzi, 53, 20125 Milano, Italy (cristina.tablinopossio@unimib.it).

ETNA
Kent State University and
Johann Radon Institute (RICAM)

be seen in the left panel of Figures 2.1, 3.1, and 4.1, where the unique univariate nondecreasing rearrangement of the symbol for $d = 2$ has a positive bounded derivative so that, in accordance with [1, Remark 4.3], the minimal eigenvalue tends to zero as N^{-1}.

When looking at the right panels of the same figures, we see the error given by the minimal distance of the eigenvalues from a very fine sampling of the spectral symbol f. In fact, since the sampling is very fine, we observe a very small error but do not see any decrease in h, which would occur when h is smaller than the stepsize in the sampling of f. For observing an error decreasing with h also for moderate h, the sampling of f should be taken with the same h as reported for the sake of clarity in Figure 2.2. Things do not change, as expected, in the variable-coefficient setting since the diffusion coefficient $a(x, y)$ is positive and bounded; see Figure 5.1.

For the rest, there is nothing much to comment given the very strong agreement of the spectral behavior of the global matrix sequences and of the corresponding approximations $\{B_{\mathbf{n},t}\}_{\mathbf{n}}$, $\{C_{\mathbf{n},t}\}_{\mathbf{n}}$ as t grows. The very striking fact is that convergence is observed already for moderate values of t, giving evidence of the practical use of the used tools, i.e., the notion of a.c.s, namely $\{\{C_{\mathbf{n},t}\}_{\mathbf{n}}\}_t$, and that, which is indeed more natural, of g.a.c.s., that is, $\{\{B_{\mathbf{n},t}\}_{\mathbf{n}}\}_t$: for the details on the approximating matrices, we refer to the left panel of Figures 2.3–2.10, 3.2–3.9, 4.2–4.9, 5.2–5.9, and compare with the left panel of Figures 2.1, 3.1, 4.1, 5.1 regarding the various matrix sequences $\{A_{\mathbf{n}}\}_{\mathbf{n}}$, respectively, while for clarifying observations we refer to [1, Remark 4.2, Section 4.2, Section 4.3]. Furthermore, in the right panel of all the Figures 2.1–5.9, the errors in the eigenvalue predictions are reported: the pseudo-random behavior can be attributed to the nondecreasing (univariate) rearrangement of the spectral symbol of $\{A_{\mathbf{n}}\}_{\mathbf{n}}$. Following the notation and the setting of the numerical experiments in [1, Section 4], the spectral symbol of the sequence $\{C_{\mathbf{n},t}\}_{\mathbf{n}}$ is given by $f_t^E(x, y, \theta_1, \theta_2) = \chi_{\Omega_t}(x, y) \cdot f$, defined on $\Omega \times [-\pi, \pi]^2)$, with f depending on the used approximation of the considered PDE. However, for simplicity in the notation, we kept the wording f_t for captions and figures regarding $\{C_{\mathbf{n},t}\}_{\mathbf{n}}$.

When maintaining the complete number of variables, a much smoother surface is expected. In addition, when looking at the figures related to the P_2-approximation, we observe 4 points where the rearranged symbol is not differentiable, and this corresponds to the 4 branches of the spectra since the symbol is 4×4 Hermitian-valued. Finally, when looking at the left panel of Figures 5.1–5.9, we observe smoother curves and wider ranges, and this is due to the variable coefficient $a(x, y)$, since each of the four eigenvalue functions in the constant coefficient case is multiplied by $a(x, y)$.

ETNA
Kent State University and
Johann Radon Institute (RICAM)

2. Finite differences/P_1-finite elements. Finite differences/P_1-finite elements symbol:

$$f(\theta_1, \theta_2) = (2 - 2\cos\theta_1) + (2 - 2\cos\theta_2).$$

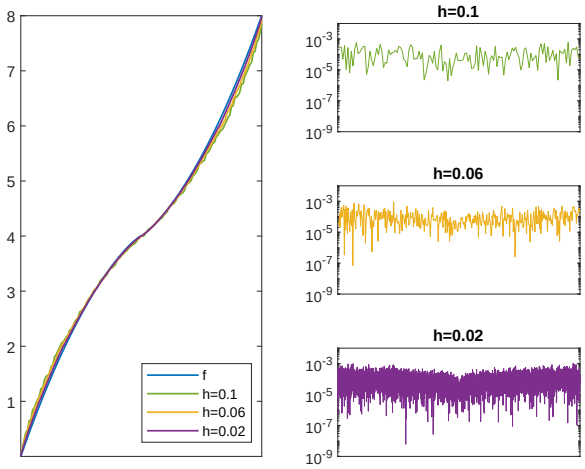

FIG. 2.1. *Left: Eigenvalue distribution of* $\{A_{\mathbf{n}}\}_{\mathbf{n}}$ *for different* h*-values together with the sampling of* $f(\theta_1, \theta_2) = (2 - 2\cos\theta_1) + (2 - 2\cos\theta_2)$*. Right: minimal distance of eigenvalues of*$A_{\mathbf{n}}$ *from* f*.*

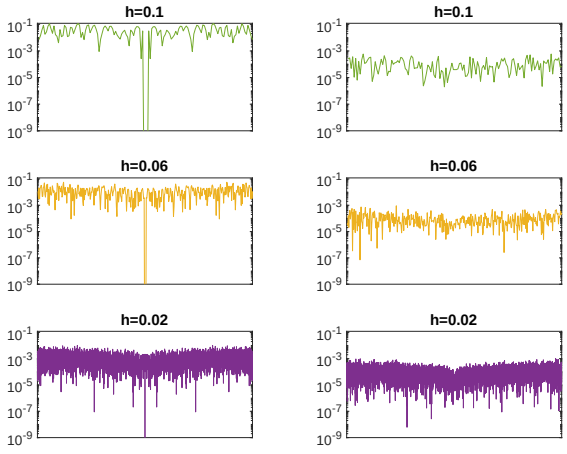

FIG. 2.2. *Minimal distance of eigenvalues of* $A_{\mathbf{n}}$ *from* $f(\theta_1, \theta_2) = (2 - 2\cos\theta_1) + (2 - 2\cos\theta_2)$ *for different* h*-values. First column with cardinality of* f *samplings comparable to eigenvalues cardinality, second column with high cardinality of* f *samplings.*

ETNA
Kent State University and
Johann Radon Institute (RICAM)

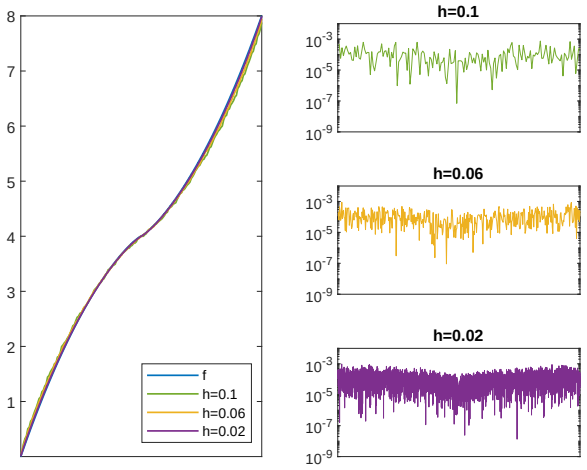

FIG. 2.3. *Left: Eigenvalue distribution of* $\{B_{\mathbf{n},t}\}_{\mathbf{n}}$ *for* $t = 2$ *and different* h*-values together with the sampling of* $f(\theta_1, \theta_2) = (2 - 2\cos\theta_1) + (2 - 2\cos\theta_2)$. *Right: minimal distance of eigenvalues of* $B_{\mathbf{n},t}$ *from* f.

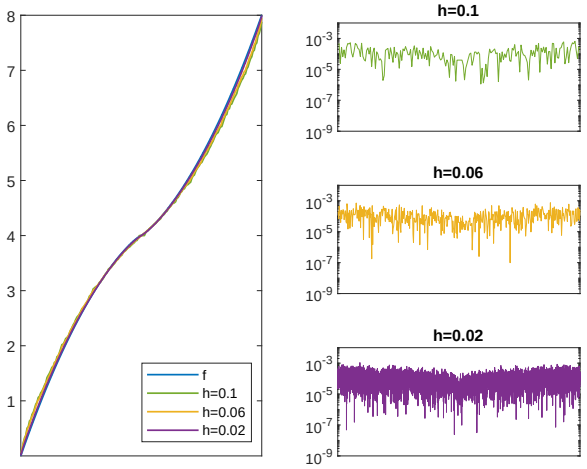

FIG. 2.4. *Left: Eigenvalue distribution of* $\{B_{\mathbf{n},t}\}_{\mathbf{n}}$ *for* $t = 4$ *and different* h*-values together with the sampling of* $f(\theta_1, \theta_2) = (2 - 2\cos\theta_1) + (2 - 2\cos\theta_2)$. *Right: minimal distance of eigenvalues of* $B_{\mathbf{n},t}$ *from* f.

ETNA
Kent State University and
Johann Radon Institute (RICAM)

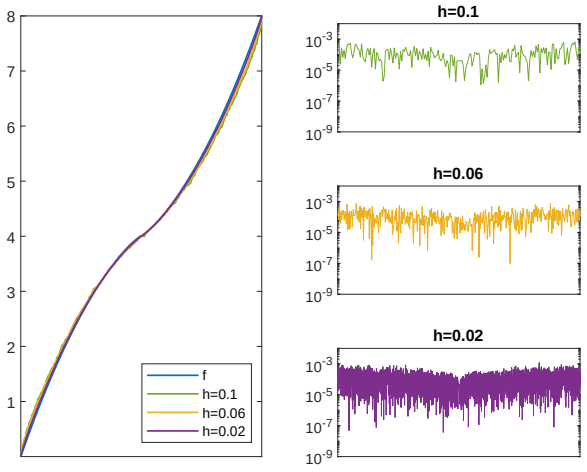

FIG. 2.5. *Left: Eigenvalue distribution of* $\{B_{\mathbf{n},t}\}_{\mathbf{n}}$ *for* $t = 6$ *and different* h*-values together with the sampling of* $f(\theta_1, \theta_2) = (2 - 2\cos\theta_1) + (2 - 2\cos\theta_2)$. *Right: minimal distance of eigenvalues of* $B_{\mathbf{n},t}$ *from* f.

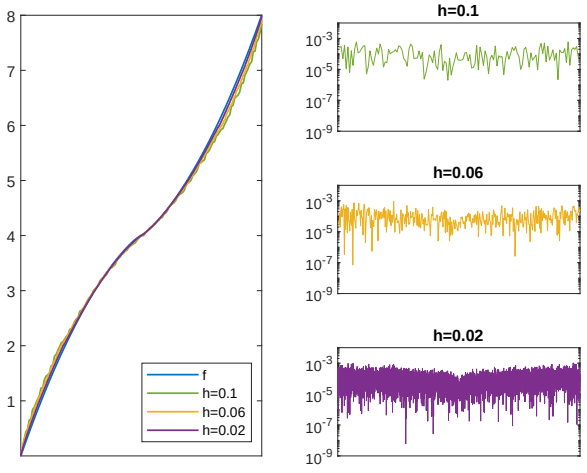

FIG. 2.6. *Left: Eigenvalue distribution of* $\{B_{\mathbf{n},t}\}_{\mathbf{n}}$ *for* $t = 8$ *and different* h*-values together with the sampling of* $f(\theta_1, \theta_2) = (2 - 2\cos\theta_1) + (2 - 2\cos\theta_2)$. *Right: minimal distance of eigenvalues of* $B_{\mathbf{n},t}$ *from* f.

ETNA
Kent State University and
Johann Radon Institute (RICAM)

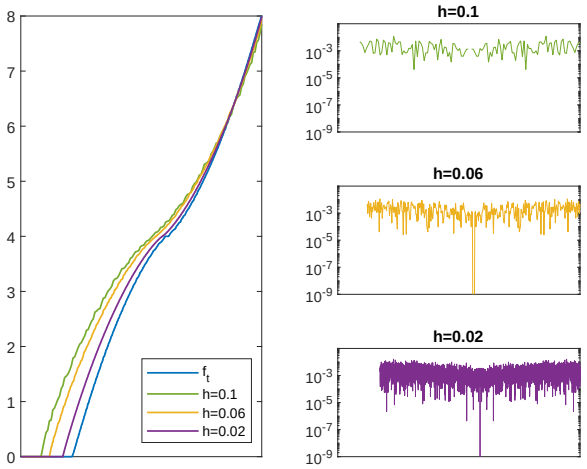

FIG. 2.7. *Left: Eigenvalue distribution of* $\{C_{\mathbf{n},t}\}_{\mathbf{n}}$ *for* $t = 2$ *and different* h*-values together with the sampling of* $f_t(x, y, \theta_1, \theta_2) = \chi_{\Omega_t}(x, y) \cdot [(2 - 2\cos\theta_1) + (2 - 2\cos\theta_2)]$. *Right: minimal distance of eigenvalues of* $C_{\mathbf{n},t}$ *from* f_t.

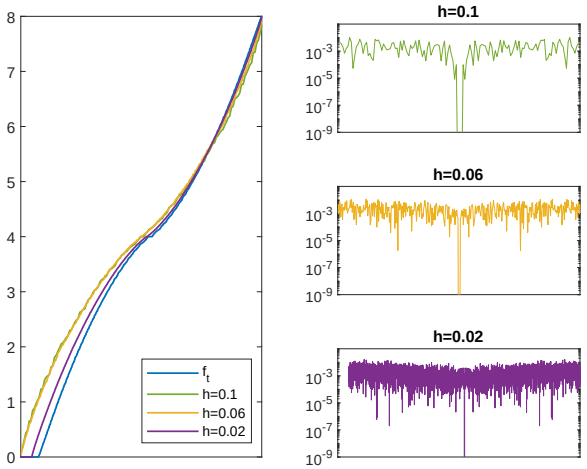

FIG. 2.8. *Left: Eigenvalue distribution of* $\{C_{\mathbf{n},t}\}_{\mathbf{n}}$ *for* $t = 4$ *and different* h*-values together with the sampling of* $f_t(x, y, \theta_1, \theta_2) = \chi_{\Omega_t}(x, y) \cdot [(2 - 2\cos\theta_1) + (2 - 2\cos\theta_2)]$. *Right: minimal distance of eigenvalues of* $C_{\mathbf{n},t}$ *from* f_t.

ETNA
Kent State University and
Johann Radon Institute (RICAM)

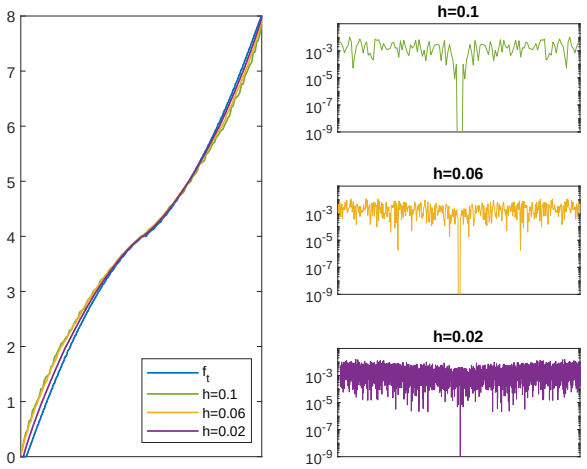

FIG. 2.9. *Left: Eigenvalue distribution of* $\{C_{\mathbf{n},t}\}_{\mathbf{n}}$ *for* $t = 6$ *and different* h*-values together with the sampling of* $f_t(x, y, \theta_1, \theta_2) = \chi_{\Omega_t}(x, y) \cdot [(2 - 2\cos\theta_1) + (2 - 2\cos\theta_2)]$. *Right: minimal distance of eigenvalues of* $C_{\mathbf{n},t}$ *from* f_t.

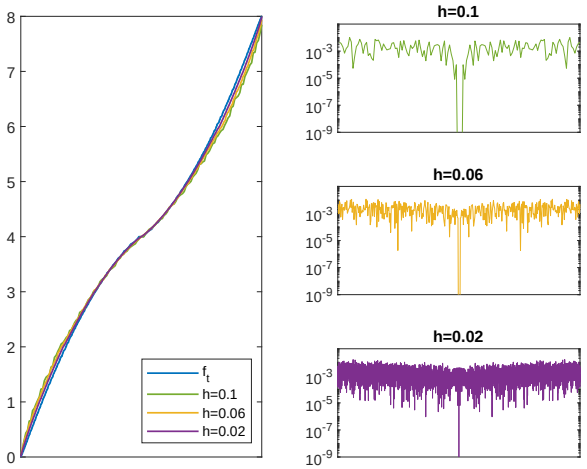

FIG. 2.10. *Left: Eigenvalue distribution of* $\{C_{\mathbf{n},t}\}_{\mathbf{n}}$ *for* $t = 8$ *and different* h*-values together with the sampling of* $f_t(x, y, \theta_1, \theta_2) = \chi_{\Omega_t}(x, y) \cdot [(2 - 2\cos\theta_1) + (2 - 2\cos\theta_2)]$. *Right: minimal distance of eigenvalues of* $C_{\mathbf{n},t}$ *from* f_t.

ETNA
Kent State University and
Johann Radon Institute (RICAM)

3. Q_1-finite elements. Q_1-finite elements symbol:

$$f(\theta_1,\theta_2) = (8 - 2\cos\theta_1 - 2\cos\theta_2 - 4\cos\theta_1\cos\theta_2)/3.$$

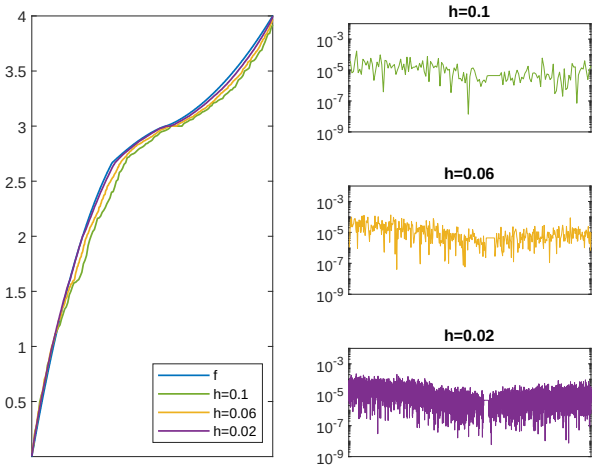

FIG. 3.1. *Left: Eigenvalue distribution of* $\{A_{\mathbf{n}}\}_{\mathbf{n}}$ *for different* h*-values together with the sampling of* $f(\theta_1,\theta_2) = (8 - 2\cos\theta_1 - 2\cos\theta_2 - 4\cos\theta_1\cos\theta_2)/3$. *Right: minimal distance of eigenvalues of* $A_{\mathbf{n}}$ *from* f.

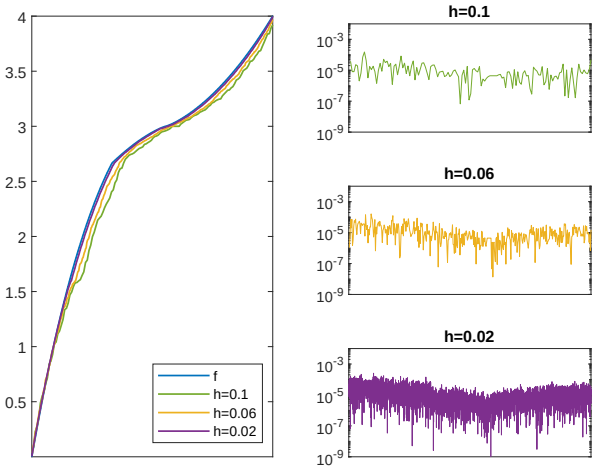

FIG. 3.2. *Left: Eigenvalue distribution of* $\{B_{\mathbf{n},t}\}_{\mathbf{n}}$ *for* $t = 2$ *and different* h*-values together with the sampling of* $f(\theta_1,\theta_2) = (8 - 2\cos\theta_1 - 2\cos\theta_2 - 4\cos\theta_1\cos\theta_2)/3$ *and (b) minimal distance of eigenvalues of* $B_{\mathbf{n},t}$ *from* f.

ETNA
Kent State University and
Johann Radon Institute (RICAM)

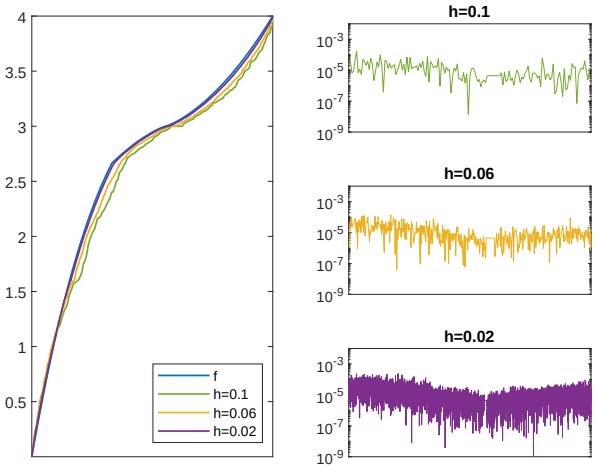

FIG. 3.3. *Left: Eigenvalue distribution of* $\{B_{\mathbf{n},t}\}_{\mathbf{n}}$ *for* $t = 4$ *and different* h*-values together with the sampling of* $f(\theta_1, \theta_2) = (8 - 2\cos\theta_1 - 2\cos\theta_2 - 4\cos\theta_1\cos\theta_2)/3$*. Right: minimal distance of eigenvalues of* $B_{\mathbf{n},t}$ *from* f.

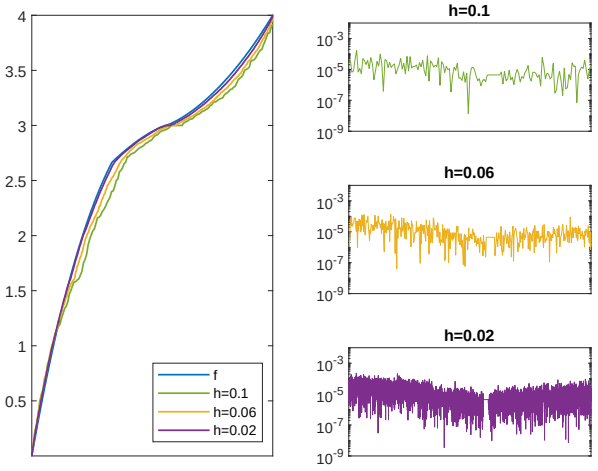

FIG. 3.4. *Left: Eigenvalue distribution of* $\{B_{\mathbf{n},t}\}_{\mathbf{n}}$ *for* $t = 6$ *and different* h*-values together with the sampling of* $f(\theta_1, \theta_2) = (8 - 2\cos\theta_1 - 2\cos\theta_2 - 4\cos\theta_1\cos\theta_2)/3$ *. Right: minimal distance of eigenvalues of* $B_{\mathbf{n},t}$ *from* f.

ETNA
Kent State University and
Johann Radon Institute (RICAM)

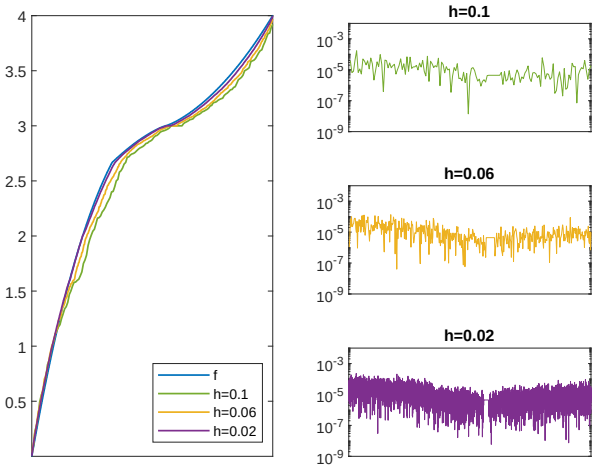

FIG. 3.5. *Left: Eigenvalue distribution of* $\{B_{\mathbf{n},t}\}_{\mathbf{n}}$ *for* $t = 8$ *and different* h*-values together with the sampling of* $f(\theta_1, \theta_2) = (8 - 2\cos\theta_1 - 2\cos\theta_2 - 4\cos\theta_1\cos\theta_2)/3$ *. Right: minimal distance of eigenvalues of* $B_{\mathbf{n},t}$ *from* f*.*

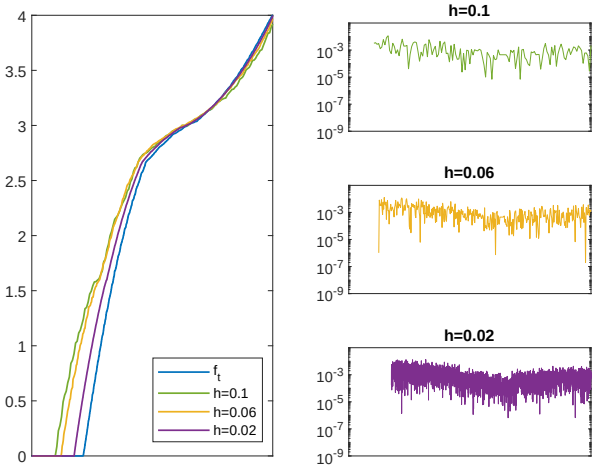

FIG. 3.6. *Left: Eigenvalue distribution of* $\{C_{\mathbf{n},t}\}_{\mathbf{n}}$ *for* $t = 2$ *and different* h*-values together with the sampling of* $f_t(x, y, \theta_1, \theta_2) = \chi_{\Omega_t}(x, y) \cdot (8 - 2\cos\theta_1 - 2\cos\theta_2 - 4\cos\theta_1\cos\theta_2)/3$*. Right: minimal distance of eigenvalues of* $C_{\mathbf{n},t}$ *from* f_t*.*

ETNA
Kent State University and
Johann Radon Institute (RICAM)

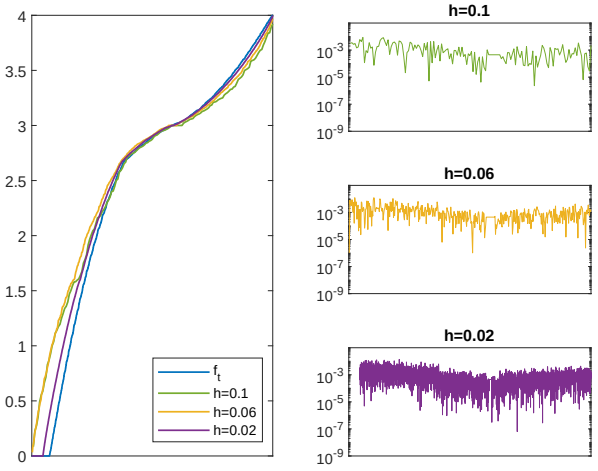

FIG. 3.7. *Left: Eigenvalue distribution of* $\{C_{\mathbf{n},t}\}_{\mathbf{n}}$ *for* $t = 4$ *and different* h*-values together with the sampling of* $f_t(x, y, \theta_1, \theta_2) = \chi_{\Omega_t}(x, y) \cdot (8 - 2\cos\theta_1 - 2\cos\theta_2 - 4\cos\theta_1\cos\theta_2)/3$*. Right: minimal distance of eigenvalues of* $C_{\mathbf{n},t}$ *from* f_t*.*

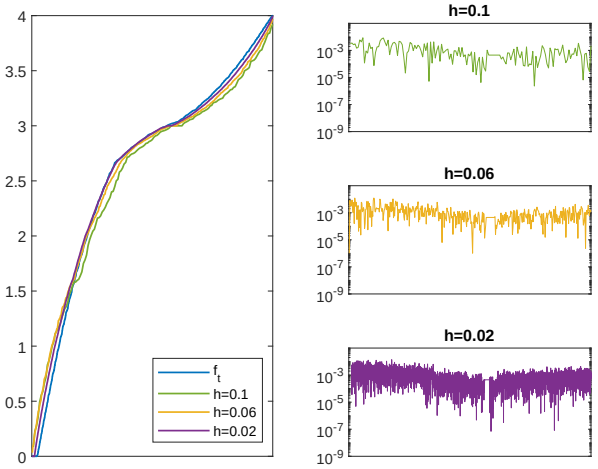

FIG. 3.8. *Left: Eigenvalue distribution of* $\{C_{\mathbf{n},t}\}_{\mathbf{n}}$ *for* $t = 6$ *and different* h*-values together with the sampling of* $f_t(x, y, \theta_1, \theta_2) = \chi_{\Omega_t}(x, y) \cdot (8 - 2\cos\theta_1 - 2\cos\theta_2 - 4\cos\theta_1\cos\theta_2)/3$*. Right: minimal distance of eigenvalues of* $C_{\mathbf{n},t}$ *from* f_t*.*

ETNA
Kent State University and
Johann Radon Institute (RICAM)

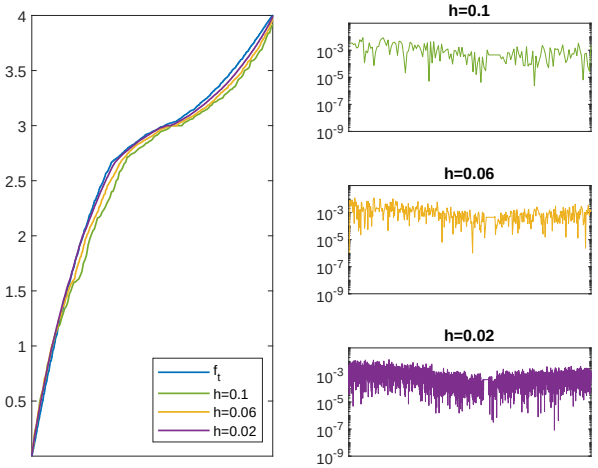

FIG. 3.9. *Left: Eigenvalue distribution of* $\{C_{\mathbf{n},t}\}_{\mathbf{n}}$ *for* $t = 8$ *and different* h*-values together with the sampling of* $f_t(x, y, \theta_1, \theta_2) = \chi_{\Omega_t}(x, y) \cdot (8 - 2\cos\theta_1 - 2\cos\theta_2 - 4\cos\theta_1\cos\theta_2)/3$*. Right: minimal distance of eigenvalues of* $C_{\mathbf{n},t}$ *from* f_t*.*

ETNA
Kent State University and
Johann Radon Institute (RICAM)

4. P_2-finite elements. P_2-finite elements matrix-valued symbol: $f_{P_2} : [-\pi, \pi]^2 \longrightarrow \mathbb{C}^{4\times 4}$ with

$$f_{P_2}(\theta_1,\theta_2) = \left[\begin{array}{cc|cc} \alpha & -\beta(1+e^{\hat{\imath}\theta_1}) & -\beta(1+e^{\hat{\imath}\theta_2}) & 0 \\ -\beta(1+e^{-\hat{\imath}\theta_1}) & \alpha & 0 & -\beta(1+e^{\hat{\imath}\theta_2}) \\ \hline -\beta(1+e^{-\hat{\imath}\theta_2}) & 0 & \alpha & -\beta(1+e^{\hat{\imath}\theta_1}) \\ 0 & -\beta(1+e^{-\hat{\imath}\theta_2}) & -\beta(1+e^{-\hat{\imath}\theta_1}) & \gamma+\frac{\beta}{2}(\cos(\theta_1)+\cos(\theta_2)) \end{array}\right],$$

with $\alpha = 16/3$, $\beta = 4/3$, and $\gamma = 4$.

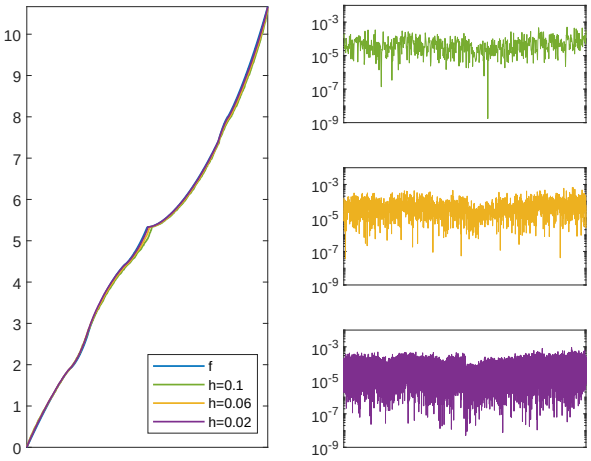

FIG. 4.1. *Left: Eigenvalue distribution of* $\{A_{\mathbf{n}}\}_{\mathbf{n}}$ *for different* h*-values together with the sampling of* $f(\theta_1,\theta_2) = f_{P_2}(\theta_1,\theta_2)$*. Right: minimal distance of eigenvalues of* $A_{\mathbf{n}}$ *from* f*.*

ETNA
Kent State University and
Johann Radon Institute (RICAM)

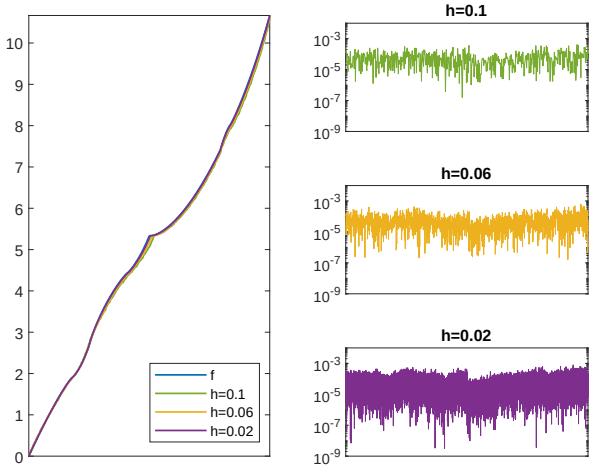

FIG. 4.2. *Eigenvalue distribution of* $\{B_{\mathbf{n},t}\}_{\mathbf{n}}$ *for* $t = 2$ *and different* h*-values together with the sampling of* $f(\theta_1, \theta_2) = f_{P_2}(\theta_1, \theta_2)$. *Right: minimal distance of eigenvalues of* $B_{\mathbf{n},t}$ *from* f.

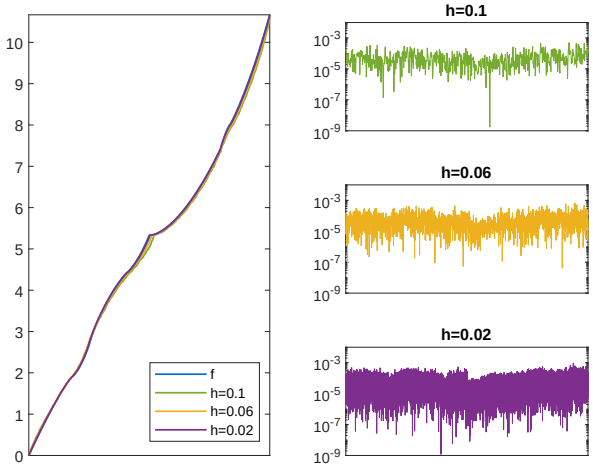

FIG. 4.3. *Left: Eigenvalue distribution of* $\{B_{\mathbf{n},t}\}_{\mathbf{n}}$ *for* $t = 4$ *and different* h*-values together with the sampling of* $f(\theta_1, \theta_2) = f_{P_2}(\theta_1, \theta_2)$. *Right: minimal distance of eigenvalues of* $B_{\mathbf{n},t}$ *from* f.

ETNA
Kent State University and
Johann Radon Institute (RICAM)

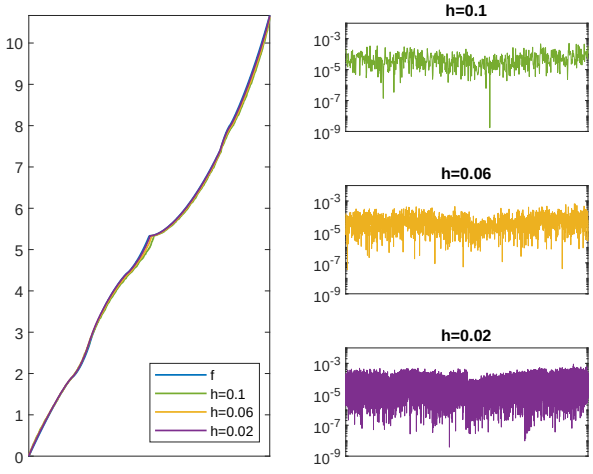

FIG. 4.4. *Left: Eigenvalue distribution of* $\{B_{\mathbf{n},t}\}_{\mathbf{n}}$ *for* $t = 6$ *and different* h*-values together with the sampling of* $f(\theta_1, \theta_2) = f_{P_2}(\theta_1, \theta_2)$*. Right: minimal distance of eigenvalues of* $B_{\mathbf{n},t}$ *from* f*.*

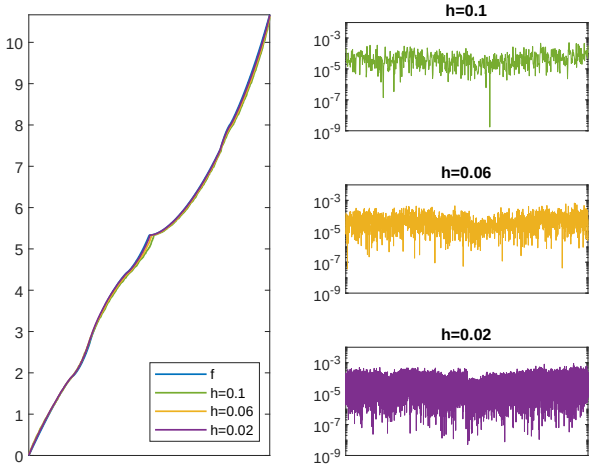

FIG. 4.5. *Left: Eigenvalue distribution of* $\{B_{\mathbf{n},t}\}_{\mathbf{n}}$ *for* $t = 8$ *and different* h*-values together with the sampling of* $f(\theta_1, \theta_2) = f_{P_2}(\theta_1, \theta_2)$*. Right: minimal distance of eigenvalues of* $B_{\mathbf{n},t}$ *from* f*.*

ETNA
Kent State University and
Johann Radon Institute (RICAM)

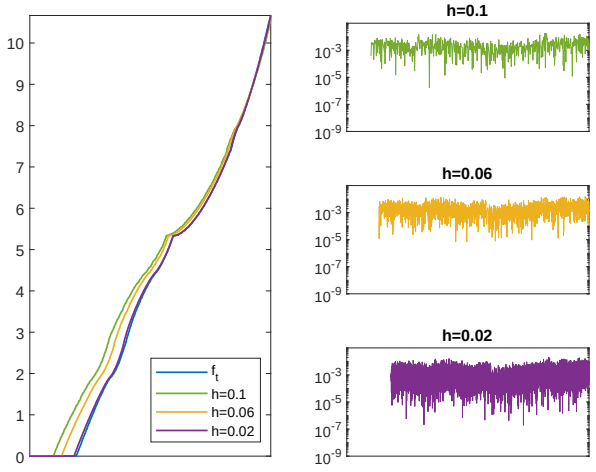

FIG. 4.6. *Left: Eigenvalue distribution of* $\{C_{\mathbf{n},t}\}_{\mathbf{n}}$ *for* $t = 2$ *and different* h*-values together with the sampling of* $f_t(x, y, \theta_1, \theta_2) = \chi_{\Omega_t}(x, y) \cdot f_{P_2}(\theta_1, \theta_2)$*. Right: minimal distance of eigenvalues of* $C_{\mathbf{n},t}$ *from* f_t*.*

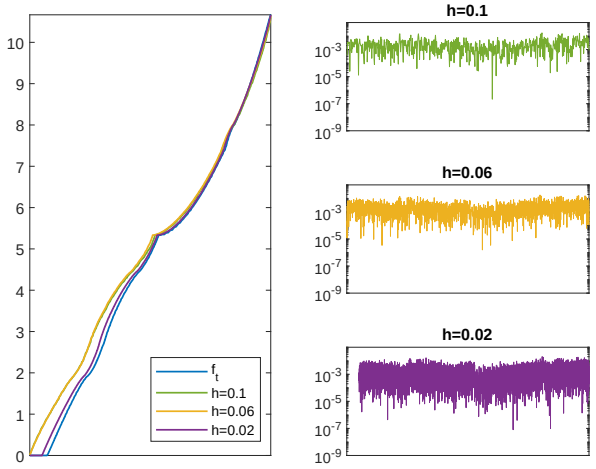

FIG. 4.7. *Left: Eigenvalue distribution of* $\{C_{\mathbf{n},t}\}_{\mathbf{n}}$ *for* $t = 4$ *and different* h*-values together with the sampling of* $f_t(x, y, \theta_1, \theta_2) = \chi_{\Omega_t}(x, y) \cdot f_{P_2}(\theta_1, \theta_2)$*. Right: minimal distance of eigenvalues of* $C_{\mathbf{n},t}$ *from* f_t*.*

ETNA
Kent State University and
Johann Radon Institute (RICAM)

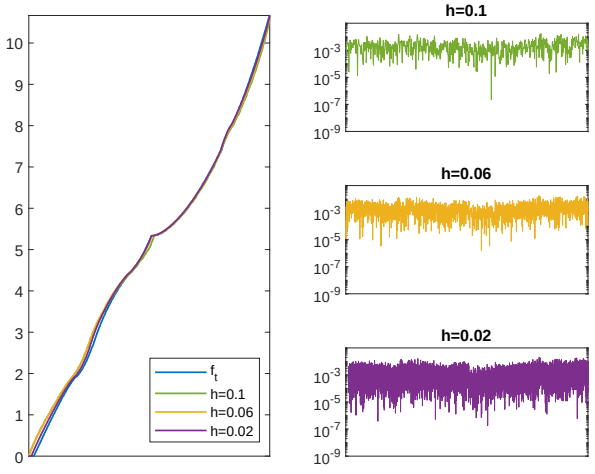

FIG. 4.8. *Left: Eigenvalue distribution of* $\{C_{\mathbf{n},t}\}_{\mathbf{n}}$ *for* $t = 6$ *and different* h*-values together with the sampling of* $f_t(x, y, \theta_1, \theta_2) = \chi_{\Omega_t}(x, y) \cdot f_{P_2}(\theta_1, \theta_2)$*. Right: minimal distance of eigenvalues of* $C_{\mathbf{n},t}$ *from* f_t*.*

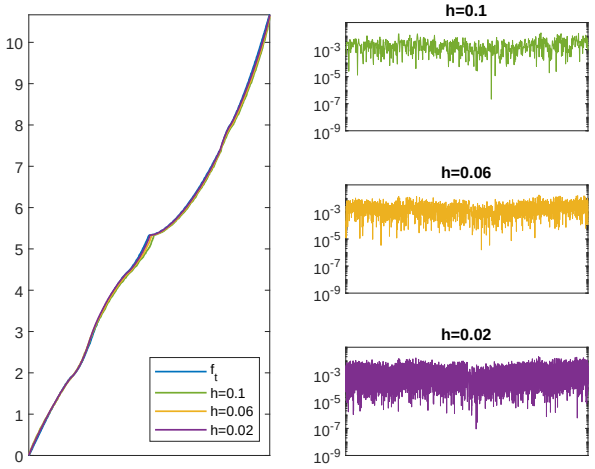

FIG. 4.9. *Left: Eigenvalue distribution of* $\{C_{\mathbf{n},t}\}_{\mathbf{n}}$ *for* $t = 8$ *and different* h*-values together with the sampling of* $f_t(x, y, \theta_1, \theta_2) = \chi_{\Omega_t}(x, y) \cdot f_{P_2}(\theta_1, \theta_2)$*. Right: minimal distance of eigenvalues of* $C_{\mathbf{n},t}$ *from* f_t*.*

ETNA
Kent State University and
Johann Radon Institute (RICAM)

5. P_1-finite elements with variable coefficient. P_1-finite elements symbol:

$$f(x,y,\theta_1,\theta_2) = a(x,y)[(2-2\cos\theta_1)+(2-2\cos\theta_2)],$$

with $a(x,y) = (10+x^2+2y^2+\sin^2(x+y))/(1+x^2+y^2)$.

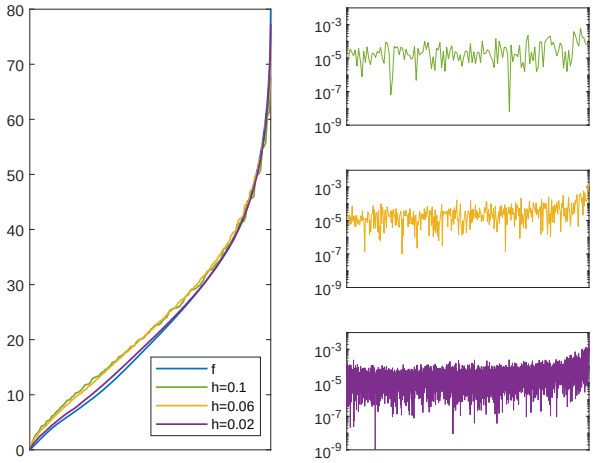

FIG. 5.1. *Left: Eigenvalue distribution of* $\{A_{\mathbf{n}}(a)\}_{\mathbf{n}}$ *for different* h*-values together with the sampling of* $f(x,y,\theta_1,\theta_2) = a(x,y)[(2-2\cos\theta_1)+(2-2\cos\theta_2)]$. *Right: minimal distance of eigenvalues of* $A_{\mathbf{n}}$ *from* f.

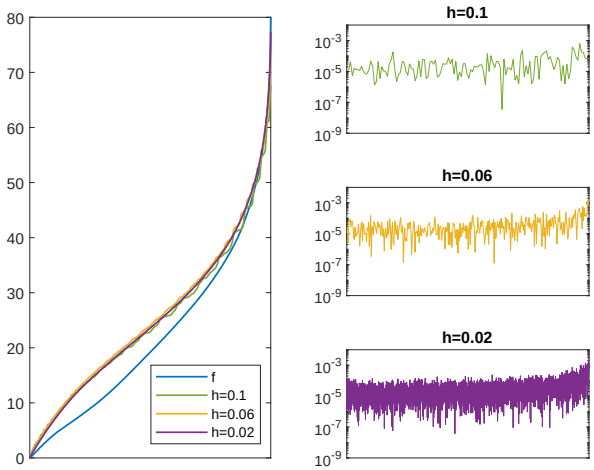

FIG. 5.2. *Left: Eigenvalue distribution of* $\{B_{\mathbf{n},t}(a)\}_{\mathbf{n}}$ *for* $t = 2$ *and different* h*-values together with the sampling of* $f(x,y,\theta_1,\theta_2) = a(x,y)[(2-2\cos\theta_1)+(2-2\cos\theta_2)]$. *Right: minimal distance of eigenvalues of* $B_{\mathbf{n},t}$ *from* f.

ETNA
Kent State University and
Johann Radon Institute (RICAM)

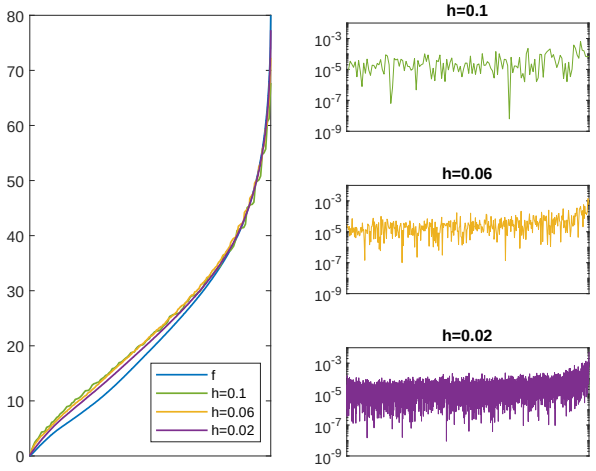

FIG. 5.3. *Left: Eigenvalue distribution of* $\{B_{\mathbf{n},t}(a)\}_{\mathbf{n}}$ *for* $t = 4$ *and different* h*-values together with the sampling of* $f(x, y, \theta_1, \theta_2) = a(x, y)[(2 - 2\cos\theta_1) + (2 - 2\cos\theta_2)]$. *Right: minimal distance of eigenvalues of* $B_{\mathbf{n},t}$ *from* f.

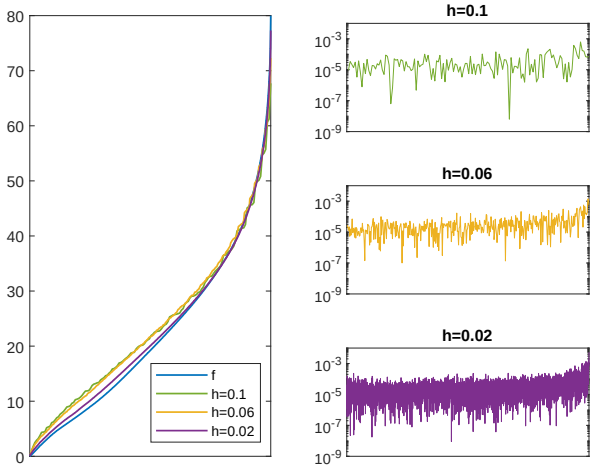

FIG. 5.4. *Left: Eigenvalue distribution of* $\{B_{\mathbf{n},t}(a)\}_{\mathbf{n}}$ *for* $t = 6$ *and different* h*-values together with the sampling of* $f(x, y, \theta_1, \theta_2) = a(x, y)[(2 - 2\cos\theta_1) + (2 - 2\cos\theta_2)]$. *Right: minimal distance of eigenvalues of* $B_{\mathbf{n},t}$ *from* f.

ETNA
Kent State University and
Johann Radon Institute (RICAM)

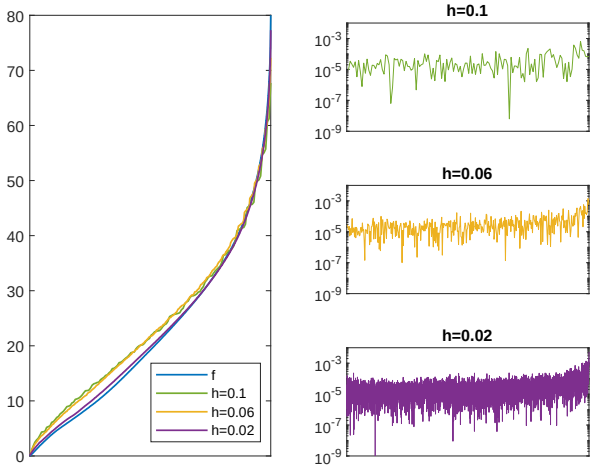

FIG. 5.5. *Left: Eigenvalue distribution of* $\{B_{\mathbf{n},t}(a)\}_{\mathbf{n}}$ *for* $t = 8$ *and different* h*-values together with the sampling of* $f(x, y, \theta_1, \theta_2) = a(x, y)[(2 - 2\cos\theta_1) + (2 - 2\cos\theta_2)]$. *Right: minimal distance of eigenvalues of* $B_{\mathbf{n},t}$ *from* f.

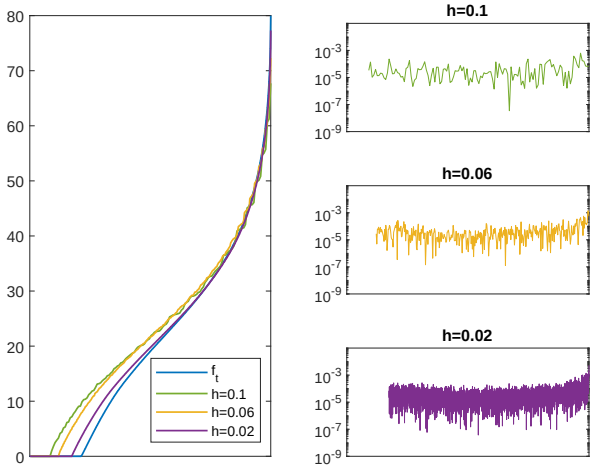

FIG. 5.6. *Left: Eigenvalue distribution of* $\{C_{\mathbf{n},t}(a)\}_{\mathbf{n}}$ *for* $t = 2$ *and different* h*-values together with the sampling of* $f_t(x, y, \theta_1, \theta_2) = \chi_{\Omega_t}(x, y)a(x, y)[(2 - 2\cos\theta_1) + (2 - 2\cos\theta_2)]$. *Right: minimal distance of eigenvalues of* $C_{\mathbf{n},t}$ *from* f_t.

ETNA
Kent State University and
Johann Radon Institute (RICAM)

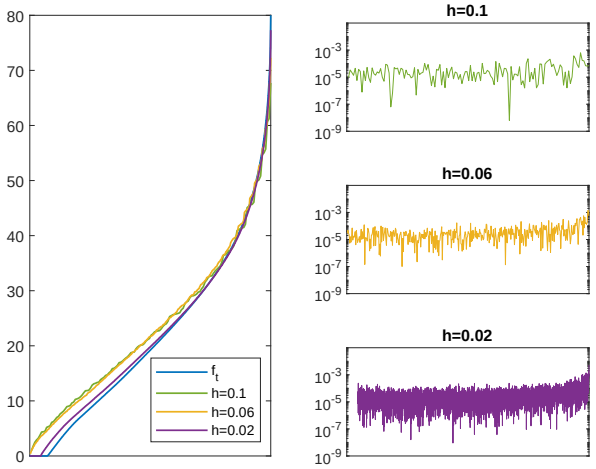

FIG. 5.7. *Left: Eigenvalue distribution of* $\{C_{\mathbf{n},t}(a)\}_{\mathbf{n}}$ *for* $t = 4$ *and different* h*-values together with the sampling of* $f_t(x, y, \theta_1, \theta_2) = \chi_{\Omega_t}(x, y)a(x, y)[(2 - 2\cos\theta_1) + (2 - 2\cos\theta_2)]$. *Right: minimal distance of eigenvalues of* $C_{\mathbf{n},t}$ *from* f_t.

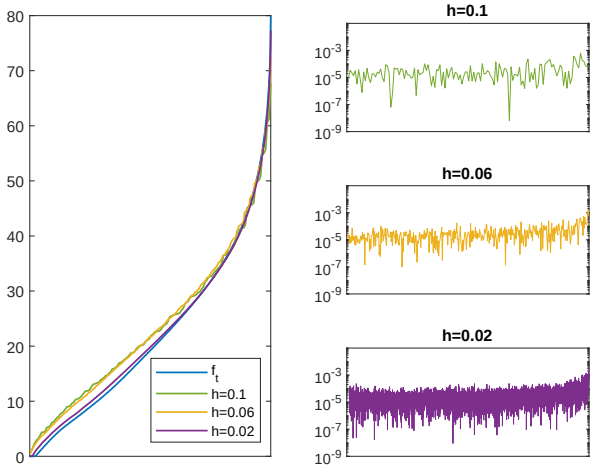

FIG. 5.8. *Left: Eigenvalue distribution of* $\{C_{\mathbf{n},t}(a)\}_{\mathbf{n}}$ *for* $t = 6$ *and different* h*-values together with the sampling of* $f_t(x, y, \theta_1, \theta_2) = \chi_{\Omega_t}(x, y)a(x, y)[(2 - 2\cos\theta_1) + (2 - 2\cos\theta_2)]$. *Right: minimal distance of eigenvalues of* $C_{\mathbf{n},t}$ *from* f_t.

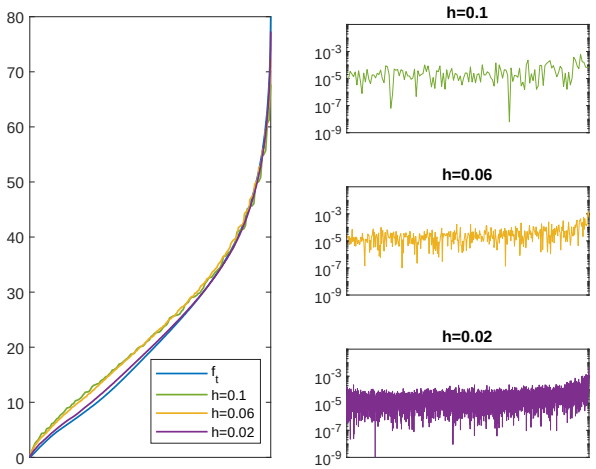

FIG. 5.9. *Left: Eigenvalue distribution of* $\{C_{\mathbf{n},t}(a)\}_{\mathbf{n}}$ *for* $t = 8$ *and different* h*-values together with the sampling of* $f_t(x, y, \theta_1, \theta_2) = \chi_{\Omega_t}(x, y)a(x, y)[(2 - 2\cos\theta_1) + (2 - 2\cos\theta_2)]$. *Right: minimal distance of eigenvalues of* $C_{\mathbf{n},t}$ *from* f_t.

REFERENCES

[1] A. ADRIANI, A. J. A. SCHIAVONI-PIAZZA, S. SERRA-CAPIZZANO, AND C. TABLINO-POSSIO, *Revisiting the notion of approximating class of sequences for handling approximated PDEs on moving or unbounded domains*, Electron. Trans. Numer. Anal., 63 (2025), pp. 424–451. https://etna.ricam.oeaw.ac.at/vol.63.2025/pp424-451.dir/pp424-451.pdf

[2] A. BÖTTCHER AND S.M. GRUDSKY, *On the condition numbers of large semidefinite Toeplitz matrices*, Linear Algebra Appl., 279 (1998), pp. 285–301.

[3] D. NOUTSOS, S. SERRA-CAPIZZANO, AND P. VASSALOS, *The conditioning of FD matrix sequences coming from semi-elliptic differential equations*, Linear Algebra Appl., 428 (2008), pp. 600–624.

[4] S. SERRA, *On the extreme spectral properties of Toeplitz matrices generated by* L^1 *functions with several minima/maxima*, BIT Numer. Math., 36 (1996), pp. 135–142.

[5] S. SERRA-CAPIZZANO, *On the extreme eigenvalues of Hermitian (block) Toeplitz matrices*, Linear Algebra Appl., 270 (1998), pp. 109–129.

[6] ———, *Distribution results on the algebra generated by Toeplitz sequences: a finite-dimensional approach*, Linear Algebra Appl., 328 (2001), pp. 121–130.

[7] P. VASSALOS, *Asymptotic results on the condition number of FD matrices approximating semi-elliptic PDEs*, Electron. J. Linear Algebra, 34 (2018), pp. 566–581.